Int J Cardiovasc Imaging (2014) 30:523–533
DOI 10.1007/s10554-014-0364-5

ORIGINAL PAPER

Three-dimensional speckle tracking echocardiography for the preclinical diagnosis of hypertrophic cardiomyopathy

Mohamed F. A. Aly · Wessel P. Brouwer · Sebastiaan A. Kleijn · Albert C. van Rossum · Otto Kamp

Received: 14 November 2013 / Accepted: 7 January 2014 / Published online: 30 January 2014

Abstract The aim is to detect early changes in myocardial mechanics in hypertrophic cardiomyopathy (HCM) mutation carriers, three-dimensional speckle tracking echocardiography (3DSTE) was used for screening of family members in the HCM population. Eighty subjects were divided as: HCM mutation carriers (n = 23), manifest HCM patients (n = 28), and normal controls (n = 29). They prospectively underwent 3DSTE for left atrial (LA) and left ventricle (LV) strain analysis. HCM mutation carriers showed significantly higher LA minimum volume (ml/m^2) (17 ± 6 vs. 14 ± 4, respectively, $P = 0.03$) and a significantly lower peak atrial longitudinal strain (PALS) (%), (27 ± 5 vs. 31 ± 7, respectively, $P = 0.02$) when compared to controls. However, no differences were found in global or regional LV systolic myocardial deformation between both groups. Manifest HCM patients, compared to carriers showed significantly higher LA minimum (27 ± 10 vs. 17 ± 6, respectively, $P < 0.001$) and maximum volume (42 ± 14 vs. 32 ± 8, respectively, $P = 0.007$) as well as lower LA ejection fraction (%) (35 ± 8 vs. 47 ± 9, respectively, $P < 0.001$) and PALS (17 ± 5 vs. 27 ± 5, respectively, $P < 0.001$). Comparing LV strain, HCM patients showed reduced global longitudinal (−11 ± 4 vs. −16 ± 3, respectively, $P < 0.001$) and area strain (−35 ±6 vs. −40 ± 5, respectively, $P = 0.005$). HCM mutation carriers may be distinguished from healthy subjects using 3DSTE through detection of LA dysfunction that may indicate LV diastolic dysfunction. Further research in a larger study population with gene-specific analysis is warranted for potential clinical usefulness of 3DSTE in family screening for HCM.

Keywords Three-dimensional echocardiography · Speckle tracking · Hypertrophic cardiomyopathy · Carrier · Left atrial function

Abbreviations

2DSTE	Two-dimensional speckle tracking echocardiography/echocardiographic
3DSTE	Three-dimensional speckle tracking echocardiography/echocardiographic
CMR	Cardiac magnetic resonance
EF	Ejection fraction
HCM	Hypertrophic cardiomyopathy
LA	Left atrium/left atrial
LV	Left ventricle/left ventricular
LVH	Left ventricular hypertrophy
PALS	Peak atrial longitudinal strain
SDI	Systolic dyssynchrony index
TDI	Tissue Doppler imaging

M. F. A. Aly (✉) · W. P. Brouwer · S. A. Kleijn · A. C. van Rossum · O. Kamp
Department of Cardiology 5F 003, Institute for Cardiovascular Research (ICaR-VU), VU University Medical Center, De Boelelaan 1117, 1081 HV Amsterdam, The Netherlands
e-mail: mfathy3@yahoo.com

M. F. A. Aly
Department of Cardiology, University Hospital, Beni-Suef, Egypt

Introduction

Hypertrophic cardiomyopathy (HCM) is the most common heritable cardiac single gene disorder and is the leading cause of sudden cardiac death in young individuals and athletes. It is most commonly caused by mutations in genes

that encode sarcomeric proteins and is characterized by unexplained left ventricular (LV) hypertrophy (LVH) [1]. However, the penetrance of mutation and expression of LVH are incomplete, highly variable, and age dependent [2]. Genetic testing provides a certain diagnosis for HCM mutation carriers before the development of LVH that may occur in these subjects. However, it is hampered by being complex and unfeasible in up to 50 % of HCM family members as genetic mutations are only identified in 40–60 % of HCM patients [3]. Therefore, an alternative family screening approach for early diagnosis of HCM patients is required. LV diastolic dysfunction as the first marker of disease in preclinical HCM mutation carriers has been previously detected by tissue Doppler imaging (TDI) [4–6]. However, the reported sensitivity and specificity were highly variable. Other techniques for the early identification of myocardial systolic dysfunction and myocardial structural alteration such as two-dimensional speckle tracking echocardiography (2DSTE) and integrated backscatter echocardiography, respectively were also investigated albeit with mixed results [6–8].Recently, cardiac magnetic resonance (CMR) imaging with its high spatial resolution has displayed subtle myocardial structural changes [9] but also intramyocardial crypts in these mainly asymptomatic patients [10]. However the availability of CMR is limited and the analysis is time consuming. Quantification of left atrial (LA) size and function is a good diagnostic tool for LV diastolic function as well as a predictor of therapy response and major cardiovascular outcomes in various cardiac patients including HCM patients [11–15]. The assessment of LA longitudinal strain using 2DSTE has recently been shown as a feasible and reproducible marker of LA function [16, 17]. Three-dimensional speckle tracking echocardiography (3DSTE) is an emerging tool building on the strengths of 2DSTE for better quantification of myocardial volumes and mechanics including assessment of dyssynchrony in one fast analysis. In this study, we tested the ability of 3DSTE to distinguish HCM mutation carriers who might develop the disease from normal subjects primarily by detecting subtle abnormalities in LA size and longitudinal strain as surrogate markers of early LV dysfunction. Likewise, we evaluated the magnitude and timing of systolic myocardial deformation to detect any abnormalities that can define early systolic dysfunction in these subjects.

Patients and methods

Patients

Based on sample size calculations, a total of 88 subjects with normal LV ejection fraction (EF) and sinus rhythm were included in the study, namely 33 patients with manifest HCM, 26 subjects with known HCM mutation carriers, and 29 normal control subjects. Manifest HCM was clinically defined as the presence of a LV maximum wall thickness (MWT) in a non-dilated LV of $\geq$15 mm or LV MWT of $\geq$13 mm as assessed by M-mode and 2DE in genotype positive patients in the absence of any systemic or other cardiac disease that could cause myocardial hypertrophy [2]. Thirty percent of the HCM patients were receiving beta-blockers and 25 %, calcium antagonists and none of them previously underwent septal reduction therapy. HCM mutation carriers were family members of HCM patients who underwent genetic testing and were found harbouring a mutation in genes encoding for any component of the sarcomere apparatus. HCM mutation carriers had LV MWT <13 mm. The normal control group (n = 29) consisted of healthy volunteers (n = 18) and healthy family members in which sarcomeric gene mutations were excluded by genetic analysis (n = 11). All HCM mutation carriers and normal controls had no history of cardiac symptoms, hypertension, diabetes or use of cardiac medication and they had normal findings on physical examination, electrocardiogram, and 2-dimensional echocardiogram. All subjects gave informed consent and the local ethics committee approved the protocol.

Echocardiographic imaging and analysis

All subjects had a complete 2DE, Doppler and TDI study using Philips iE33 with S5-1 Matrix transducer. Furthermore, they all prospectively underwent 3DSTE examination on the same sitting of the 2DE study using a commercial scanner (Artida 4D, Toshiba Medical Systems, Tokyo, Japan) with a fully sampled matrix array transducer (PST–25SX) from an apical position for both LV and LA analysis. Eight subjects (10 %) were excluded after echocardiographic acquisitions due to either poor LV image quality (defined as >4 non-visualised segments) (n = 6) or very low volume rate of acquisition (<11 vpm) (n = 2). Image quality of the LA was sufficient for all subjects and was not a reason for exclusion. In tissue harmonic mode, wide-angled acquisitions were recorded consisting of four wedge-shaped sub-volumes acquired over five consecutive cardiac cycles during a single breath-hold. While retaining the entire LV within the pyramidal volume, depth and sector width were decreased as much as possible to improve the temporal and spatial resolution of the images, resulting in a mean temporal resolution of 21 $\pm$ 3 volumes per second. Analysis of 3DSTE for the LA and LV was done as previously described [18]. The LV mass is automatically calculated after epicardial and endocardial contour detection. The obtained 3DSTE strain data for the LV included three conventional strain components (circumferential, radial and,

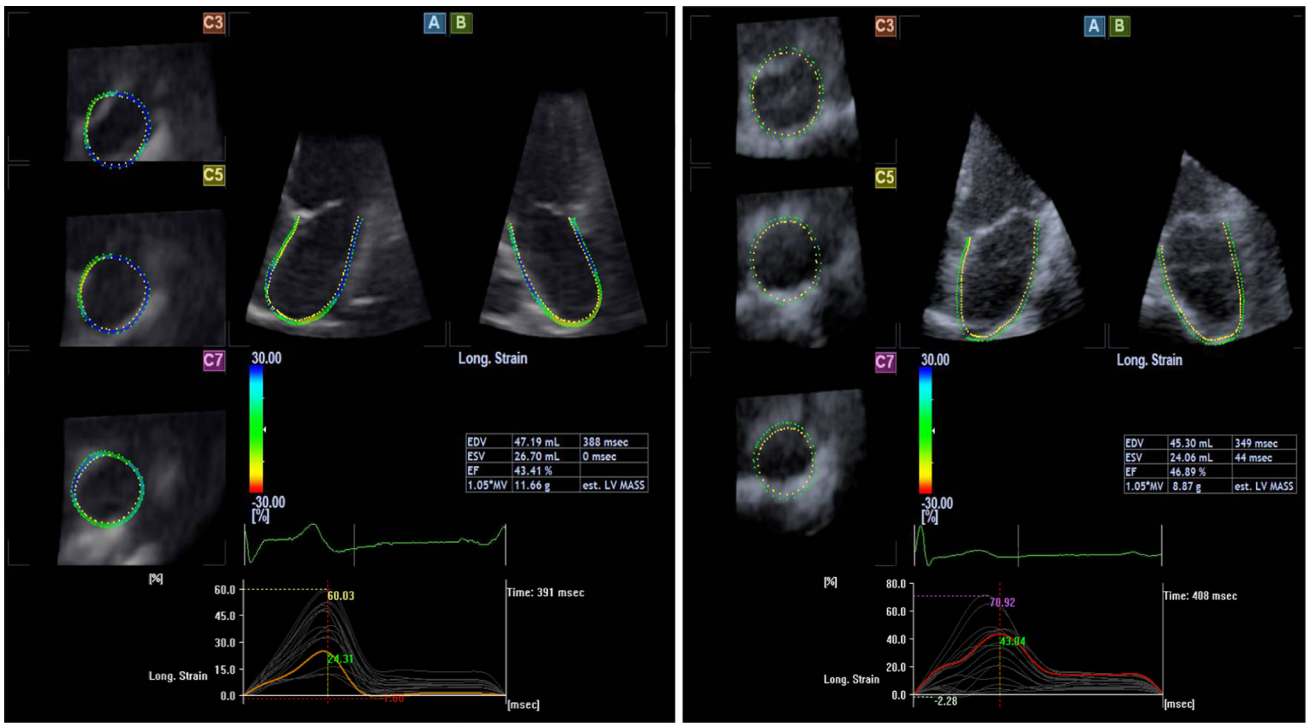

Fig. 1 Left atrial longitudinal strain analysis using 3DSTE. Tracing of the LA endocardial border is performed from the base of the LA at the mitral valve level toward the LA apex, while excluding the LA appendage and the pulmonary veins from the LA cavity. Tracing was done in apical four-chamber view (*A*), apical two-chamber view (*B*), and three short axis planes (*C3, C5, C7*). The frame of LV end-systole with maximum LA volume is presented for a carrier (*left*) and a normal control (*right*). The showed *curves* represent the segmental longitudinal strains with the coloured one showing the global longitudinal strain where the PALS is in the carrier is lower (24 %) compared to the normal control (43 %) with comparable LA volumes

longitudinal) as well as area strain as a novel global strain parameter. The area strain was calculated as the endocardial area change ratio throughout the cardiac cycle by giving the percentage decrease in area at LV end-systole from its original dimensions at end-diastole. Systolic dyssynchrony index (SDI%) was used to quantify the LV mechanical dyssynchrony. It was calculated as the standard deviation (SD) of the timings to peak strain of the 16 LV segments and given as a percentage of the cardiac cycle duration after normalization for the R–R duration. Peak atrial longitudinal strain (PALS) represents the maximum reservoir function of the LA where LA strain increases due to stretch by accumulating venous blood. It achieves a peak at the end of LA filling just before mitral valve opening. PALS can be used as a measure of LA relaxation and as it corresponds to the phases of LV from end-diastole to end-systole namely; LV isovolumic contraction, ejection, and isovolumic relaxation; it is sometimes described as peak LA ventricular systolic strain. During diastasis, LA strain decreases to reach a negative peak at the end of LA contraction. The 3DSTE software automatically calculates the PALS by measuring the peak positive strain from the QRS onset and averages the global PALS value from each of the 16 LA segments (Fig. 1). Other LA longitudinal strains representing the LA conduit and pump functions were not measured as they need manual calculations guided by the ECG and this would be unreliable.

Observer reliability

Observer reliability to evaluate PALS as a novel 3DSTE-derived parameter was assessed in a randomly selected number of 15 manifest HCM patients. 3DSTE data sets were analysed for inter-observer reliability by two experienced observers (M.F. and S.K.) in a blinded fashion. Intra-observer measures were performed on average 2 weeks apart in random order. The observer reliability of 3DSTE-derived LV strain components were extensively studied in a previous study that included HCM patients [18].

Statistical analysis

Continuous variables are presented as mean ± SD, whereas categorical variables are presented as frequencies and percentages. One-way analysis of variance was used to examine the differences among groups with Bonferroni's correction for multiple pair-wise comparisons. Differences in continuous variables between two groups were analysed using the student's *t* test, while a Chi square test or the

Fisher exact test was used to analyze a difference in categorical variables as appropriate. Inter-observer and intra-observer reliability were measured using the intra-class correlation coefficient (ICC). To determine the ICC, different variance components were calculated using restricted maximum likelihood method of estimation and a model for absolute agreement, where the observers and patients were entered as random effects. A P value <0.05 was considered statistically significant. All data were analysed using SPSS version 20.0 (IBM SPSS Inc., Chicago, IL, USA).

Results

Baseline and echocardiographic characteristics

As displayed in Table 1, the HCM mutation carriers were well matched for age and body surface area (BSA) with the normal controls as these are important determinant of LA strain [16]. Due to the bigger BSA in manifest HCM patients, the indexed 3DSTE LA volumes, LV volumes and mass were used. There was no matching for gender between HCM carriers and normal controls. By definition, LV MWT was significantly higher in the manifest HCM group compared with other groups. For the distribution of gene mutation, myosin binding protein C3 (*MYBPC3*) was the most predominant mutation in both HCM mutation carriers (66 %) and manifests HCM patients (39 %). Other carriers equally had troponin T mutation (17 %) or myosin heavy chain mutation (*MYH7*) (17 %). Based on 2DE, the majority of manifest HCM (79 %) had no obstruction and the remaining 6 patients had fixed and/or dynamic obstruction. Eighteen patients (64 %) had asymmetrical septal hypertrophy. Both HCM mutation carriers and controls showed similar normal mitral inflow Doppler indices. However for the mitral annular TD velocities, HCM mutation carriers, compared to controls; showed significantly lower lateral and averaged Ea. In addition, HCM mutation carriers showed significantly higher lateral, septal, and averaged E/Ea as surrogates of LV filling pressure. When compared to manifest HCM patients, HCM mutation carriers showed significantly higher both lateral and averaged Sa and Ea and septal Ea as well. They also showed a significantly lower lateral, septal, and averaged E/Ea and Pulmonary capillary wedge pressure (PCWP), which is calculated by the echo machine as a surrogate of LA pressure using the Ea parameters. By applying the ROC curve analysis to test the discriminatory power of any of these statically different Doppler parameters, the area under the curve was insufficient (<0.5) to yield a good sensitivity and specificity to differentiate HCM mutation carriers from normals.

LA analysis

In HCM mutation carriers compared to normal controls, LA minimum volume (LAV_{min}) was significantly higher (17 ± 6 vs. 14 ± 4, respectively, $P = 0.03$) and PALS was significantly lower (27 ± 5 vs. 31 ± 7, respectively, $P = 0.02$) whereas the LA maximum volume (LAV_{max}) and LA EF did not show a significant difference as shown in Table 2 and Fig. 1. Using the ROC curve analysis to test the discriminatory power of LAV_{min} and PALS to differentiate HCM mutation carriers from normals, the area under the curve for both was insufficient (0.40 and 0.33, respectively) to yield a reasonable sensitivity and specificity. Compared to manifest HCM patients, HCM mutation carriers showed a significantly lower LAV_{min} and LAV_{max} and a significantly higher LAEF and PALS as shown in Table 2. When correlating 3DSTE LA parameters to the TD mitral annular velocities and L V parameters, only PALS that could show a significant moderate correlation with lateral and averaged Ea as well as LV longitudinal strain ($r = 0.58$, 0.63, and 0.60, $P < 0.001$ for all, respectively) whereas there were poor correlations between any of the mitral annular TD velocities and different LV parameters ($r < 0.50$).

LV analysis

By comparing HCM mutation carriers to normal controls, there were no significant differences in LV volumes, LVEF or LV mass. In addition, the global LV strain parameters namely circumferential, radial, and longitudinal strain as well as area strain and their derived SDI did not differ between both groups as seen in Table 2. Furthermore, no significant differences could be detected in any of these strain parameters on a segmental level as shown in Table 3. Of note, even the basal anterior septum where hypertrophy most commonly manifests, did not show significant difference in LV strain components including the longitudinal strain (-14 ± 6 vs. -15 ± 8 %, respectively, $P = 0.4$).

Manifest HCM patients on the other hand showed a significantly lower LV end-diastolic volume and a higher LV mass compared to HCM mutation carriers as seen in Table 2. In addition, the global longitudinal strain and area strain were considerably impaired despite the presence of a normal LVEF; the global longitudinal strain was reduced by 31 % (-11 ± 4 vs. -16 ± 3 %, respectively, $P < 0.001$), and area strain was reduced by 13 % (-35 ± 6 vs. -40 ± 5 %, respectively, $P = 0.005$) as detailed in Table 2 and Fig. 2. No significant difference in the global circumferential or radial strain between both groups was found. For the assessment of mechanical dyssynchrony, only the longitudinal strain-derived SDI was significantly higher in manifest HCM patients. On a regional level, all myocardial

Table 1 Baseline population and echocardiographic characteristics

Variable	Normal controls (n = 29)	Carriers HCM (n = 23)	Manifest HCM (n = 28)	*P* value All groups	*P* value Carriers versus controls	*P* value Carriers versus manifest	*P* value Manifest versus controls
Age (y)	46 ± 16	41 ± 15	54 ± 16	0.007	0.2	0.002	0.06
Men (%)	23 (79)	6 (26)	21 (75)	<0.001	<0.001	<0.001	0.8
BSA (kg/m^2)	1.8 ± 0.12	1.8 ± 0.13	2 ± 0.2	<0.001	0.2	0.005	0.06
LVMWT (mm)	9.1 ± 1.1	9.4 ± 2	18 ± 3	<0.001	0.5	<0.001	<0.001
Mitral Doppler inflow indices							
E (cm/s)	73 ± 15	71 ± 17	67 ± 18	0.6	0.7	0.6	0.3
A (cm/s)	56 ± 14	60 ± 15	74 ± 34	0.03	0.4	0.08	0.02
E/A ratio	1.4 ± 0.5	1.3 ± 0.4	1 ± 0.4	0.01	0.3	0.1	0.01
Deceleration time (ms)	186 ± 50	197 ± 40	206 ± 40	0.3	0.5	0.4	0.1
Mitral annular TD velocities							
Lateral wall (cm/s)							
Sa	10.4 ± 2.3	9.8 ± 2.6	7 ± 2	<0.001	0.4	<0.001	<0.001
Ea	13 ± 2.9	10.8 ± 3.7	8.2 ± 2.4	<0.001	0.04	0.02	<0.001
Aa	9 ± 2.4	9.5 ± 2.9	9.4 ± 3.6	0.9	0.6	0.9	0.7
E/Ea	5.7 ± 1.5	7 ± 2.2	8.9 ± 3.1	<0.001	0.03	0.03	<0.001
Septal wall (cm/s)							
Sa	8.5 ± 1.7	7.9 ± 1.1	7 ± 2.3	0.03	0.2	0.1	0.02
Ea	9.3 ± 2	7.9 ± 2.7	5.3 ± 1.6	<0.001	0.06	0.001	<0.001
Aa	8 ± 1.5	8.9 ± 1.7	7.5 ± 2	0.04	0.07	0.02	0.4
E/Ea	8.3 ± 1.6	9.4 ± 2	14.3 ± 5.5	<0.001	0.04	<0.001	<0.001
Averaged (cm/s)							
Sa	9.5 ± 1.7	8.8 ± 1.7	7 ± 2	<0.001	0.2	0.004	<0.001
Ea	11.2 ± 2.2	9.3 ± 3	6.8 ± 1.9	<0.001	0.03	0.003	<0.001
Aa	8.5 ± 1.8	9.2 ± 2.1	8.5 ± 2.6	0.5	0.2	0.3	0.9
E/Ea	6.9 ± 1.4	8 ± 2	11 ± 4	<0.001	0.03	0.004	<0.001
PCWP	9.1 ± 1.8	10.2 ± 2.7	13.7 ± 5.3	<0.001	0.07	0.02	<0.001

Values are presented as mean ± SD or absolute number (percentage)

BSA body surface area, *LVMWT* left ventricular maximum wall thickness, *E* early rapid filling wave, *A* filling wave due to atrial contraction, *Sa* systolic annular velocity, *Ea* early diastolic annular velocity, *Aa* late diastolic annular velocity, *PCWP* pulmonary capillary wedge pressure as a surrogate of left atrial pressure

P value <0.05 is significant

walls had lowers longitudinal strain values particularly in the septum which was decreased by one-third (−10 ± 4 vs. −15 ± 3 %, respectively, $P < 0.001$). In addition, the area strain was lower in the septum and lateral walls. Regional circumferential and radial strains as well as area strain in the anterior and inferior walls were not different between both groups as in Table 3.

Observer reliability

Inter-observer and intra-observer reliability for both LA volumes and PALS were good whereas they were moderate for LA EF as displayed in Table 4.

Discussion

Echocardiography has clinical advantages, including its availability, time and cost-efficiency, and ease of use in most patients and clinical settings. 3DSTE by addressing the limitations of 2DSTE may become the technique of choice for clinical evaluation of LV and LA size and function in daily routine [18–20]. Currently, there is a pressing clinical need of finding a feasible and accurate imaging tool as an alternative approach to gene testing to detect subtle abnormalities that might exist in relatives of HCM patients for the preclinical diagnosis of this serious disease, which would be of a great importance. In this regard, this is the first study using 3DSTE for the

Table 2 Global left atrial and ventricular analysis using 3DSTE

Variable	Normal controls (n = 29)	Carriers HCM (n = 23)	Manifest HCM (n = 28)	*P* value All groups	*P* value Carriers versus controls	*P* value Carriers versus manifest	*P* value Manifest versus controls
3DE image quality (n)	1*(20) and 2*(9)	1*(19) and 2*(4)	1*(16) and 2*(12)	0.2	0.2	0.05	0.5
3DE volume rate (vps)	23 ± 12	21 ± 3	21 ± 3	0.4	0.6	0.4	0.3
Heart rate (bpm)	69 ± 11	67 ± 10	65 ± 12	0.4	0.5	0.5	0.2
LA analysis							
$LAVI_{min}$ (ml/m^2)	14 ± 4	17 ± 6	27 ± 10	<0.001	0.03	<0.001	<0.001
$LAVI_{max}$ (ml/m^2)	28 ± 7	32 ± 8	42 ± 14	<0.001	0.07	0.007	<0.001
LAEF (%)	50 ± 11	47 ± 9	35 ± 8	<0.001	0.3	<0.001	<0.001
PALS (%)	31 ± 7	27 ± 5	17 ± 5	<0.001	0.02	<0.001	<0.001
LV analysis							
LV volumes and mass							
LVEDVI (ml/m^2)	56 ± 12	54 ± 9	48 ± 12	0.03	0.6	0.04	<0.001
LVESVI (ml/m^2)	23 ± 6	23 ± 5	21 ± 6	0.4	0.8	0.2	<0.001
LVEF (%)	59 ± 5	57 ± 5	57 ± 4	0.2	0.1	0.98	0.3
LV MassI (g/m^2)	65 ± 15	65 ± 9	84 ± 24	<0.001	0.9	<0.001	0.002
LV strain (%)							
Circumferential strain	−29 ± 4	−28 ± 4	−26 ± 6	0.2	0.6	0.3	0.09
Longitudinal strain	−15 ± 3	−16 ± 3	−11 ± 4	<0.001	0.6	<0.001	<0.001
Radial strain	32 ± 9	30 ± 10	27 ± 9	0.08	0.5	0.2	0.03
Area strain	−40 ± 4	−40 ± 5	−35 ± 6	0.001	0.9	0.005	0.001
LV dyssynchrony (%)							
Circumferential strain SDI	5.3 ± 2.7	5.1 ± 1.9	5.5 ± 2.4	0.9	0.8	0.5	0.7
Longitudinal strain SDI	7.6 ± 4.8	8.3 ± 4	13 ± 7	0.001	0.6	0.007	0.002
Radial strain SDI	8.6 ± 3.7	9 ± 3.4	13.3 ± 11.6	0.05	0.7	0.09	0.05
Area strain SDI	4.6 ± 1.9	4.7 ± 1.9	4.8 ± 1.7	0.9	0.9	0.9	0.7

*1**, good; *2**, moderate

LVEDVI indexed left ventricular end-diastolic volume, *LVESVI* indexed left ventricular end-systolic volume, *LVEF* left ventricular ejection fraction, *LV MassI* indexed left ventricular mass, $LAVI_{min}$ indexed left atrial minimum volume, $LAVI_{max}$ indexed left atrial maximum volume, *LAEF* left atrial ejection fraction, *PALS* peak atrial longitudinal strain

P value <0.05 is significant

evaluation of both functional and structural changes across the entire phenotypic spectrum of HCM. The main result is that 3DSTE in HCM mutation carriers as supported by TDI findings was able to detect indirect markers of LV diastolic dysfunction in the form of an increase in LA size and a decrease in PALS. Compared to normal subjects, no significant differences in LV systolic function in this group were found.

Assessment of LA size and function

LA dilatation and the decrease in its EF have been shown to be good diagnostic signs of LV diastolic dysfunction and markers of poor prognosis of different cardiovascular diseases [17]. LA reservoir function was shown to be determined by integration of LA wall relaxation and both LV systolic and diastolic function. LA wall state should have an effect on LA relaxation and reservoir function in its early part [21, 22]. LV systolic function influences the LA reservoir function through mitral annulus descent from the LV base to apex during late systole [22]. Elevated LV end-diastolic pressure causes LA contractile dysfunction and remodelling of the LA due to increased afterload during LA contraction. This LA contractile dysfunction causes LA relaxation impairment due to the coupling present between LA systolic dysfunction and relaxation. In addition, the LA remodelling causes thickening of the LA wall. Both mechanisms end with impaired PALS [23, 24]. Measuring LA volumes by 3DSTE was shown to be a feasible and reproducible in a large study [18]. It has been demonstrated that 2DSTE-derived PALS is a feasible and reproducible marker of the LA deformation that may be more sensitive than LAEF in detecting early impairment of the LA reservoir function [16, 17]. Moreover, 3DSTE-derived LA

Table 3 Regional left ventricular strain analysis using 3DSTE

Variable	Normal controls (n = 29)	Carriers HCM (n = 23)	Manifest HCM (n = 28)	*P* value All groups	*P* value Carriers versus controls	*P* value Carriers versus manifest	*P* value Manifest versus controls
Regional circumferential strain (%)							
Anterior	−25 ± 5	−26 ± 5	−26 ± 5	0.6	0.4	0.98	0.4
Septal	−31 ± 6	−29 ± 6	−27 ± 6	0.02	0.1	0.3	0.006
Inferior	−28 ± 6	−30 ± 5	−27 ± 8	0.2	0.4	0.1	0.4
Lateral	−30 ± 7	−29 ± 7	−27 ± 5	0.2	0.6	0.3	0.07
Regional longitudinal strain (%)							
Anterior	−15 ± 4	−15 ± 4	−11 ± 4	<0.001	0.7	0.002	<0.001
Septal	−15 ± 3	−15 ± 3	−10 ± 4	<0.001	0.8	<0.001	<0.001
Inferior	−16 ± 4	−18 ± 4	−13 ± 4	<0.001	0.1	<0.001	0.007
Lateral	−17 ± 3	−18 ± 4	−13 ± 4	<0.001	0.9	<0.001	<0.001
Regional radial strain (%)							
Anterior	37 ± 17	33 ± 15	30 ± 17	0.3	0.4	0.5	0.2
Septal	33 ± 11	33 ± 9	26 ± 12	0.04	0.9	0.06	0.02
Inferior	30 ± 12	30 ± 10	27 ± 13	0.4	0.8	0.4	0.3
Lateral	40 ± 17	35 ± 19	32 ± 11	0.2	0.4	0.4	0.06
Regional area strain (%)							
Anterior	−38 ± 7	−36 ± 8	−35 ± 9	0.4	0.6	0.5	0.2
Septal	−41 ± 5	−40 ± 6	−34 ± 8	<0.001	0.9	0.007	<0.001
Inferior	−41 ± 5	−40 ± 5	−37 ± 7	0.03	0.3	0.08	0.01
Lateral	−44 ± 5	−42 ± 8	−37 ± 6	0.001	0.9	0.02	<0.001

P value <0.05 is significant

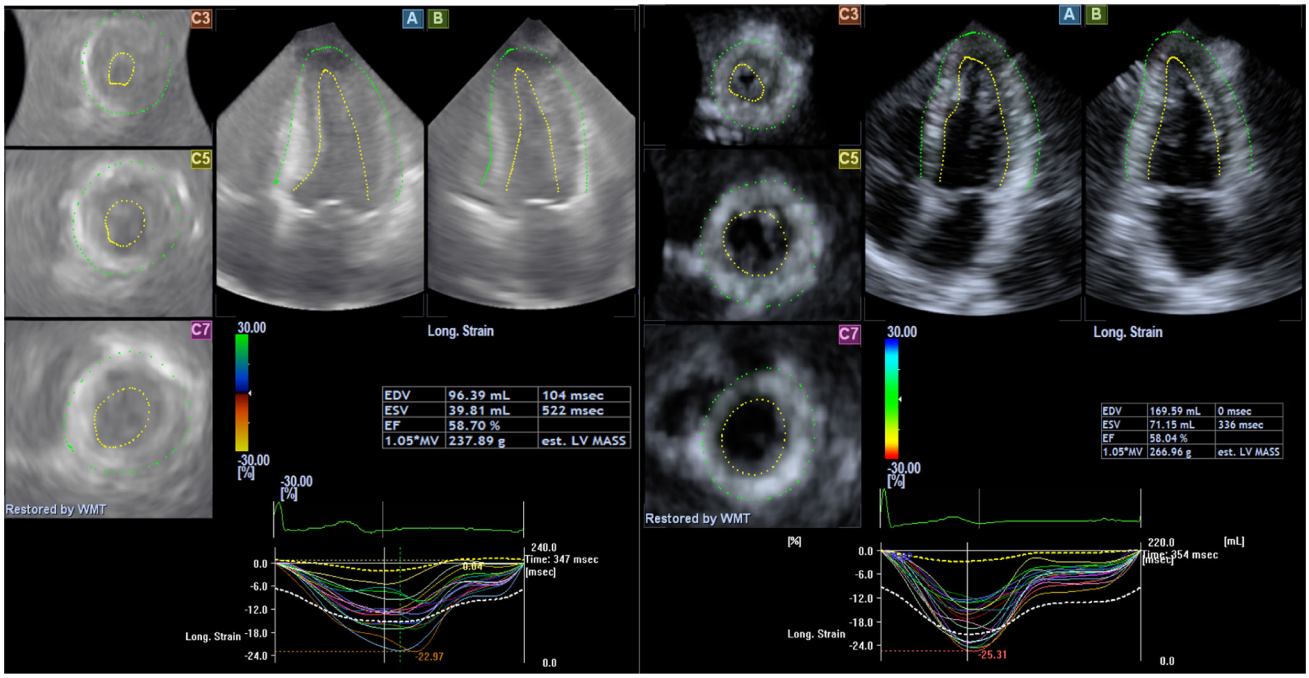

Fig. 2 Left ventricular longitudinal strain analysis using 3DSTE. After 3DSTE semiautomated border detection and tracking, LV volumes, mass and EF are quantified in a manifest HCM patient (*left*) and a normal control (*right*). The showed *curves* represent the segmental longitudinal strains. The *dashed curve* represents the average strain which is lower in the manifest HCM patient (−7 %) compared to the normal control (−13 %)

Table 4 Intra-observer and inter-observer reliability of LA measurements

Variable	Intra-observer reliability		Inter-observer reliability	
	ICC	*P* value	ICC	*P* value
$LAVI_{min}$ (ml/m^2)	0.88	<0.001	0.80	<0.001
$LAVI_{max}$ (ml/m^2)	0.89	<0.001	0.84	<0.001
LAEF (%)	0.67	<0.001	0.61	0.006
PALS (%)	0.88	<0.001	0.83	<0.001

ICC intra-class correlation coefficient

P value <0.05 is significant

longitudinal strain has been recently demonstrated feasible as well, and more reproducible and beneficial than 2DSTE longitudinal strain for identifying patients with paroxysmal atrial fibrillation [25]. In the present study, we used 3DSTE to study the LA volume and also PALS as a substitute of LA volume change in the evaluation of LA reservoir function in HCM as an indirect marker of both LV diastolic and systolic function.

Our results revealed that 3DSTE gives reproducible quantification of LA volumes, and PALS as a new 3DSTE-derived parameter is highly reproducible with a better reproducibility than LA EF. This data are consistent with larger feasibility studies for LA volume quantification [18] and PALS assessment [25] using 3DSTE. Our reported normal values of PALS are higher than those given by Mochizuki et al. [25] (31 ± 8 vs. 26 ± 7 %, respectively); however this could be explained by the lower mean age in our group (48 ± 15 vs. 58 ± 5 years, respectively). Both LAV_{max} and LAV_{min} were significantly dilated, and LAEF were significantly reduced in manifest HCM patients as compared to both HCM mutation carriers and normal subjects. This finding is consistent with the results of previous studies reported enlarged LAV in manifest HCM patients [11]. The reduced PALS measured by 3DSTE in our study was also similar to the reported impaired PALS measured by 2DSTE in manifest HCM patients [12–15].

One of the aims of the current study was to focus on these indirect LA markers of LV impairment in the group of HCM mutation carriers. We could define a significantly dilated LAV_{min} and reduced PALS in this group compared to normal controls, albeit none of them was able to have a clinically applied sensitivity and specificity due to the wide overlap between their values in mutation carriers and controls. The dilated LAV_{min} and the decreased PALS in the HCM mutation carriers could be related to the presence of LV diastolic dysfunction as detected by TDI that might precede LV systolic dysfunction. Since the impairment of LV diastolic function in this group is subtle, the changes in the LAV_{min} and PALS were not evident, especially for the PALS which is mainly related to the LV systolic function which was completely preserved in this group. The LAV_{min} has been shown recently to be a better correlate of LV diastolic dysfunction and to be more sensitive than LAV_{max}. This is because the LAV_{min} is more directly exposed to LV pressure through an open mitral valve than LAV_{max}. The latter is only affected by the LV longitudinal systolic function through the systolic descent of the mitral annulus towards the apex during systole with subsequent stretch of the LA [26]. As long as both the diastolic and systolic LV impairment were more evident and long standing in the manifest HCM compared to HCM mutation carriers, the LAV_{min} got more dilated and the PALS became more significantly reduced. In addition, the LAV_{max} was dilated and the LAEF was reduced. Furthermore, this reported LA dysfunction could be due to a primary LA affection caused by the generalized myopathic process in HCM affecting both atrial and ventricular myocardium [11, 13].

Assessment of LV size and function

The histopathologic changes of the myocardium in HCM lead to both LV diastolic and systolic dysfunction. LV diastolic dysfunction is secondary to a reduction of LV compliance (increased LV mass) and increased stiffness (myocardial fibrosis) which is coupled to a decrease of ventricular volume as a contributing factor. The systolic dysfunction is due to the impaired active force generation and contractile dysfunction despite the clinically hyperdynamic systolic function secondary to decreased afterload as a result of the small LV cavity [27]. Furthermore, the observed LV dyssynchrony in our study as a significantly increased longitudinal strain-derived SDI despite normal QRS duration may be another reason for the impaired contractility and subsequent heterogeneity of relaxation and this adds to our understanding of the myocardial mechanics in HCM. The impaired long-axis function appears as a more sensitive marker for myocardial pathology and reveals earlier impairment of the cardiac function [28]. This can be explained by the fact that longitudinal function is mainly related to the subendocardial fibres which are more susceptible to the perfusion abnormalities and affected by the interstitial fibrosis [29]. In the current study, in agreement with previous studies in patients with HCM, LV diastolic dysfunction is evident [11–14]. In view of systolic function assessment and compared to previous studies using 2DSTE strain [6–8, 30–32] tagged CMR [33] and 3DSTE [34], the longitudinal strain as a representative of long-axis function was the most reduced strain parameter both globally and regionally in addition to the presence of longitudinal dyssynchrony. The significantly low radial strain observed in our study is also consistent with previous results [10, 31, 33] although

one study reported a normal radial strain [7]. The results for the circumferential strain are somewhat contradictory. While in our study and similarly to others [7] it was preserved, it was decreased in others [8, 29, 30] and increased in yet another study which might be a compensatory response to maintain the systolic dysfunction [33]. The contradictory results among studies concerning their radial and circumferential LV strain values might be linked to using different echocardiography machines as recently reported by Banado et al. [35] using two different 3DSTE vendors. Our results also revealed a significantly reduced area strain which represents a global motion of deformation, not available in 2D imaging. This finding may be an evidence for the diverse phenotypic patterns of altered myocardial mechanics seen in patients with HCM.

In view of these diastolic and systolic strain abnormalities observed in manifest HCM patients, we tried to detect similar abnormalities in the carrier group. Compared to normal controls, our results revealed subtle LV diastolic dysfunction as denoted from TDI parameters in the HCM mutation carriers and this finding is consistent with the results of previous studies using different measures of LV diastolic function like Doppler mitral, pulmonary inflow, and TDI [7–10]. These results further support the clinical importance of the TD mitral annular velocities as an easy to perform and widely available clinical echocardiographic tool to assess the LV diastolic function. The diastolic dysfunction is assumed to be due to the intrinsic functional consequences of sarcomere mutations and the early pathologic changes in the myocardium before the development of cardiac hypertrophy. On the other hand, our results did not support the presence of any global or regional systolic strain abnormalities in those HCM mutation carriers. These negative results are consistent with prior reports used 2DSTE for the absence of global systolic impairment [6–8] and for the absence of regional systolic abnormalities as well [7]. However, our results differ from other studies on the regional level with regard to the involvement of the basal anterior septum. Whereas our study does not demonstrate any difference of systolic function in that region, others reported a decreased longitudinal strain using 2DSTE [6, 8] or an increased calibrated integrated backscatter using backscatter echocardiography [8]. These contradictory results in HCM mutation carriers might be explained by different gene mutations that vary with respect to their pathogenesis and age dependent penetrance [36]. Therefore, a family member who is assumed to be a mutation carrier might indeed carry a non-disease causing variant and show normal echocardiographic indices including indices of LA strain. One study compared two age-adjusted cohorts of HCM mutation carriers with the most commonly prevalent mutations, namely; *MYH7* and *MYBPC3*. It reported that subjects with *MYH7* mutations had evidence of more impaired diastolic function, but enhanced regional systolic function relative to subjects with *MYBPC3* mutations. The proposed explanation given for this exaggerated myocardial contractility in regions experiencing higher longitudinal strain may be a compensatory mechanism to sarcomeric mutations that paradoxically precede the development of LVH [7]. Therefore, longitudinal studies to follow preclinical sarcomere mutation carriers over time are needed to fully describe the temporal sequence of phenotypic evolution.

Study limitations

An important limitation of the current study is the relatively small number of subjects in each group. Accordingly, comparing different types of gene mutations in the HCM mutation carriers was not possible and this precludes the universal application of these results to studies with different distribution of mutations. Absence of matching for gender between HCM carriers and normal controls remains a limitation even after adjustment for other baseline characteristics. Likewise, we could not define the effect of obstruction and the medications on the strain values in manifest HCM patients. Another limitation was that the LA was analysed using software created for LV quantification as a dedicated software package for the LA analysis has not been released yet.

Conclusions

HCM mutation carriers may be distinguished from healthy subjects using 3DSTE through detection of LA dysfunction that may indicate LV diastolic dysfunction. However, single parameters have insufficient diagnostics yield to be clinically useful on their own. Further research in a larger study population with gene-specific analysis is warranted to demonstrate the potential clinical usefulness of 3DSTE with its ongoing future development in family screening for HCM.

Conflict of interest None.

References

1. Abdel-Aty H, Zagrosek A, Schulz-Menger J, Taylor AJ, Messroghli D, Kumar A, Gross M, Dietz R, Friedrich MG (2004) Delayed enhancement and T2-weighted cardiovascular magnetic resonance imaging differentiate acute from chronic myocardial infarction. Circulation 109(20):2411–2416
2. Gersh BJ, Maron BJ, Bonow RO et al (2011) 2011 ACCF/AHA guideline for the diagnosis and treatment of hypertrophic cardiomyopathy: a report of the American College of Cardiology

Foundation/American Heart Association Task Force on practice guidelines. Circulation 124(24):2761–2796
3. Ho CY, Seidman CE (2006) A contemporary approach to hypertrophic cardiomyopathy. Circulation 113(24):858–862
4. Nagueh SF, Bachinski LL, Meyer D, Hill R, Zoghbi WA, Tam JW, Quiñones MA, Roberts R, Marian AJ (2001) Tissue Doppler imaging consistently detects myocardial abnormalities in patients with hypertrophic cardiomyopathy and provides a novel means for an early diagnosis before and independently of hypertrophy. Circulation 104(2):128–130
5. Ho CY, Sweitzer NK, McDonough B, Maron BJ, Casey SA, Seidman JG, Seidman CE, Solomon SD (2002) Assessment of diastolic function with Doppler tissue imaging to predict genotype in preclinical hypertrophic cardiomyopathy. Circulation 105(25):2992–2997
6. Sabe De, Borowski AG, Wang H, Nye L, Xin B, Thomas JD, Tang WH (2011) Subclinical echocardiographic abnormalities in phenotype-negative carriers of myosin-binding protein C3 gene mutation for hypertrophic cardiomyopathy. Am Heart J 162(2): 262–267
7. Ho CY, Carlsen C, Thune JJ et al (2009) Echocardiographic strain imaging to assess early and late consequences of sarcomere mutations in hypertrophic cardiomyopathy. Circ Cardiovasc Genet 2(4):314–321
8. Yiu KH, Atsma DE, Delgado V et al (2012) Myocardial structural alteration and systolic dysfunction in preclinical hypertrophic cardiomyopathy mutation carriers. PLoS ONE 7(5):36115
9. Germans T, Wilde AA, Dijkmans PA, Chai W, Kamp O, Pinto YM, van Rossum AC (2006) Structural abnormalities of the inferoseptal left ventricular wall detected by cardiac magnetic resonance imaging in carriers of hypertrophic cardiomyopathy mutations. J Am Coll Cardiol 48(12):2518–2523
10. Brouwer WP, Germans T, Head MC, van der Velden J, Heymans MW, Christiaans I, Houweling AC, Wilde AA, van Rossum AC (2012) Multiple myocardial crypts on modified long-axis view are a specific finding in pre-hypertrophic HCM mutation carriers. Eur Heart J Cardiovasc Imaging 13(4):292–297
11. Yang H, Woo A, Monakier D, Jamorski M, Fedwick K, Wigle ED, Rakowski H (2005) Enlarged left atrial volume in hypertrophic cardiomyopathy: a marker for disease severity. J Am Soc Echocardiogr 18(10):1074–1082
12. Gabrielli L, Enriquez A, Cordova S, Yanez F, Godoy I, Corbalan R (2012) Assessment of left atrial function in hypertrophic cardiomyopathy and athlete's heart: a left atrial myocardial deformation study. Echocardiography 29(8):943–949
13. Rosca M, Popescu BA, Beladan CC et al (2010) Left atrial dysfunction as a correlate of heart failure symptoms in hypertrophic cardiomyopathy. J Am Soc Echocardiogr 23(10):1090–1098
14. Prinz C, Van Buuren F, Bogunovic N, Bitter T, Faber L, Horstkotte D (2012) In patients with hypertrophic cardiomyopathy myocardial fibrosis is associated with both left ventricular and left atrial dysfunction. Acta Cardiol 67(2):187–193
15. Paraskevaidis IA, Farmakis D, Papadopoulos C, Ikonomidis I, Parissis J, Rigopoulos A, Iliodromitis EK, Kremastinos DT (2009) Two-dimensional strain analysis in patients with hypertrophic cardiomyopathy and normal systolic function: a 12-month follow-up study. Am Heart J 158(3):444–450
16. Saraiva RM, Demirkol S, Buakhamsri A, Greenberg N, Popović ZB, Thomas JD, Klein AL (2010) Left atrial strain measured by two-dimensional speckle tracking represents a new tool to evaluate left atrial function. J Am Soc Echocardiogr 23(2):172–180
17. Mor-Avi V, Lang RM, Badano LP et al (2011) Current and evolving echocardiographic techniques for the quantitative evaluation of cardiac mechanics: aSE/EAE consensus statement on methodology and indications endorsed by the Japanese Society of Echocardiography. J Am Soc Echocardiogr 24(3):277–313
18. Kleijn SA, Aly MF, Terwee CB, van Rossum AC, Kamp O (2011) Comparison between direct volumetric and speckle tracking methodologies for left ventricular and left atrial chamber quantification by three-dimensional echocardiography. Am J Cardiol 108(7):1038–1044
19. Kleijn SA, Aly MF, Terwee CB, van Rossum AC, Kamp O (2012) Reliability of left ventricular volumes and function measurements using three-dimensional speckle tracking echocardiography. Eur Heart J Cardiovasc Imaging 13(2):159–168
20. Kleijn SA, Brouwer WP, Aly MF, Rüssel IK, de Roest GJ, Beek AM, van Rossum AC, Kamp O (2012) Comparison between three-dimensional speckle-tracking echocardiography and cardiac magnetic resonance imaging for quantification of left ventricular volumes and function. Eur Heart J Cardiovasc Imaging 13(10): 834–839
21. Oki T, Tabata T, Yamada H, Fukuda K, Abe M, Onose Y, Wakatsuki T, Iuchi A, Ito S (1998) Assessment of abnormal left atrial relaxation by transesophageal pulsed Doppler echocardiography of pulmonary venous flow velocity. Clin Cardiol 21(10): 753–758
22. Barbier P, Solomon SB, Schiller NB, Glantz SA (1999) Left atrial relaxation and left ventricular systolic function determine left atrial reservoir function. Circulation 100(4):427–436
23. Wakami K, Ohte N, Asada K, Fukuta H, Goto T, Mukai S, Narita H, Kimura G (2009) Correlation between left ventricular end-diastolic pressure and peak left atrial wall strain during left ventricular systole. J Am Soc Echocardiogr 22(7):847–851
24. Yoshida T, Ohte N, Narita H, Sakata S, Wakami K, Asada K, Miyabe H, Saeki T, Kimura G (2006) Lack of inertia force of late systolic aortic flow is a cause of left ventricular isolated diastolic dysfunction in patients with coronary artery disease. J Am Coll Cardiol 48(5):983–991
25. Mochizuki A, Yuda S, Oi Y et al (2013) Assessment of left atrial deformation and synchrony by three-dimensional speckle-tracking echocardiography: comparative studies in healthy subjects and patients with atrial fibrillation. J Am Soc Echocardiogr 26(2):165–174
26. Russo C, Jin Z, Homma S, Rundek T, Elkind MS, Sacco RL, Di Tullio MR (2012) Left atrial minimum volume and reservoir function as correlates of left ventricular diastolic function: impact of left ventricular systolic function. Heart 98(10):813–820
27. Hughes SE (2004) The pathology of hypertrophic cardiomyopathy. Histopathology 44(5):412–427
28. Rajiv C, Vinereanu D, Fraser AG (2004) Tissue Doppler imaging for the evaluation of patients with hypertrophic cardiomyopathy. Curr Opin Cardiol 19(5):430–436
29. Popović ZB, Kwon DH, Mishra M, Buakhamsri A, Greenberg NL, Thamilarasan M, Thomas JD, Lever HM, Desai MY (2008) Association between regional ventricular function and myocardial fibrosis in hypertrophic cardiomyopathy assessed by speckle tracking echocardiography and delayed hyperenhancement magnetic resonance imaging. J Am Soc Echocardiogr 21(12):1299–1305
30. Carasso S, Yang H, Woo A, Vannan MA, Jamorski M, Wigle ED, Rakowski H (2008) Systolic myocardial mechanics in hypertrophic cardiomyopathy: novel concepts and implications for clinical status. J Am Soc Echocardiogr 21(6):675–683
31. Sun JP, Stewart WJ, Yang XS, Donnell RO, Leon AR, Felner JM, Thomas JD, Merlino JD (2009) Differentiation of hypertrophic cardiomyopathy and cardiac amyloidosis from other causes of ventricular wall thickening by two-dimensional strain imaging echocardiography. Am J Cardiol 103(3):411–415
32. Soullier C, Obert P, Doucende G, Nottin S, Cade S, Perez-Martin A, Messner-Pellenc P, Schuster I (2012) Exercise response in hypertrophic cardiomyopathy: blunted left ventricular deformational and twisting reserve with altered systolic-diastolic coupling. Circ Cardiovasc Imaging 5(3):324–332

33. Dong SJ, MacGregor JH, Crawley AP, McVeigh E, Belenkie I, Smith ER, Tyberg JV, Beyar R (1994) Left ventricular wall thickness and regional systolic function in patients with hypertrophic cardiomyopathy. A three-dimensional tagged magnetic resonance imaging study. Circulation 90(3):1200–1209
34. Baccouche H, Maunz M, Beck T, Gaa E, Banzhaf M, Knayer U, Fogarassy P, Beyer M (2012) Differentiating cardiac amyloidosis and hypertrophic cardiomyopathy by use of three-dimensional speckle tracking echocardiography. Echocardiography 29(6):668–677
35. Badano LP, Cucchini U, Muraru D, Al Nono O, Sarais C, Iliceto S (2013) Use of three dimensional speckle tracking to assess left ventricular myocardial mechanics: inter-vendor consistency and reproducibility of strain measurements. Eur Heart J Cardiovasc Imaging 14(3):285–293
36. Xin B, Puffenberger E, Tumbush J, Bockoven JR, Wang H (2007) Homozygosity for a novel splice site mutation in the cardiac myosin-binding protein C gene causes severe neonatal hypertrophic cardiomyopathy. Am J Med Genet A 143A(22):2662–2667